Kidney claudin-19: Localization in distal tubules and collecting ducts and dysregulation in polycystic renal disease

Nikki P.Y. Lee[a], Man K. Tong[a], Pauline P. Leung[a], Vivian W. Chan[a], Simon Leung[a], Po-Chor Tam[a], Kwok-Wah Chan[b], Kai-Fai Lee[c], William S.B. Yeung[c], John M. Luk[a,*]

[a] Department of Surgery, Queen Mary Hospital, The University of Hong Kong, Pokfulam, Hong Kong, SAR, China
[b] Department of Pathology, Queen Mary Hospital, The University of Hong Kong, Pokfulam, Hong Kong, SAR, China
[c] Department of Obstetrics and Gynaecology, Queen Mary Hospital, The University of Hong Kong, Pokfulam, Hong Kong, SAR, China

Abstract Tight junction (TJ) constitutes the barrier by controlling the passage of ions and molecules via paracellular pathway and the movement of proteins and lipids between apical and basolateral domains of the plasma membrane. Claudins, occludin, and junctional adhesion molecules are the major three transmembrane proteins at TJ. This study focuses a newly identified mammalian TJ gene, claudin-19, in kidneys. Mouse claudin-19 composes of 224 amino acids and shares 98.2% and 95% amino acid homology with rat and human, respectively; the most evolutionary-related claudins are claudin-1 and -7, which share ∼75% DNA sequence homology with claudin-19. Claudin-19 is abundantly expressed in the mouse and rat kidneys among the organs examined by Northern blots, and to a much less extent, also found in brain by RT-PCR. Claudin-19 and zonula occludens-1 (ZO-1) are localized at junctional regions of Madin–Darby canine kidney (MDCK) cells by immunofluorescent microscopy. In addition, ZO-1 is found in the claudin-19-associated protein complexes in MDCK cells by co-immunoprecipitation. Using aquaporin-1 and aquaporin-2 antibodies as markers for different renal segment, strong expression of claudin-19 was observed in distal tubules of the cortex as well as in the collecting ducts of the medulla. To less extent, claudin-19 is also present in the proximal tubules (cortex) and in the loop of Henle (medulla). Furthermore, intense claudin-19 immunoreactivity is found co-localized with the ZO-1 in kidneys from postnatal day 15, day 45, and adult rats and mice. Similar localizations of claudin-19 and ZO-1 are also observed in human kidneys. Since these renal segments are mainly for controlling the paracellular cation transport, it is suggested that claudin-19 may participate in these processes. In human polycystic kidneys, decreased expression and dyslocalization of claudin-19 are noticed, suggesting a possible correlation between claudin-19 and renal disorders. Taken together, claudin-19 is a claudin isoform that is highly and specifically expressed in renal tubules with a putative role in TJ homeostasis in renal physiology.
© 2006 Federation of European Biochemical Societies. Published by Elsevier B.V. All rights reserved.

Keywords: Aquaporins; Claudin-19; Kidney; Polycystic disease; Tight junction

1. Introduction

Cell–cell interaction is crucial for tissue patterning and morphogenesis as well as homeostasis of normal tissues. Structural integrity of normal epithelia is maintained by junctional complexes, such as tight junctions (TJs) [1,2]. TJ fibrils are composed of three major transmembrane proteins, namely claudins, occludin, and junctional adhesion molecules (JAMs) [1,2]. Among them, claudin constitutes the largest TJ protein family with at least 24 claudins identified, whereas only two occludins and three JAMs [1,3,4] are found. All claudins are predicted to have molecular weights ranging between 20 and 27 kDa [1,4]. Structurally, each claudin has two extracellular loops, one intracellular loop, one intracellular carboxyl- (C-) and one intracellular amino- (N-) terminus. In particular, the last several amino acids of the C-terminus constitute PDZ-binding motifs. The two extracellular loops form adhesive contacts lining the TJ seals [4]. Functionally, TJ forms physical barriers in epithelia and endothelia to regulate paracellular transports of ions, water, and molecules by discriminating sizes and charges [5].

Kidney functions as a filter unit and an osmoregulator in the body by regulating the body's fluid volume and mineral/solute composition partly via paracellular transport. It accomplishes these roles by the presence of segmented nephrons, such as proximal tubules, with specific and diverse properties. For instance, proximal tubules are regarded as 'leaky' segments, whereas distal tubules are termed as the 'tight' portions along the renal nephrons [6]. To fine-tune the paracellular transport in renal nephrons, kidneys are equipped with a large number of claudins and each claudin demonstrates diversified renal distributions. For instance, all claudins, except claudin-6, -9, -13, and -14, are found in total kidney extracts by Northern blot analysis [7]. Claudin-2, -10, and -11 are situated at the proximal tubules, whereas claudin-3, -7, and -8 are found in the distal tubules [7–9]. In particular, claudin-2 restricted in proximal tubules is only expressed in Madin–Darby canine kidney (MDCK) II cells (with low transepithelial electrical resistance), but not MDCK I cells (with high transepithelial electrical resistance) [9–11], demonstrating the specific roles of claudin-2 in maintaining the 'leaky' TJ in proximal tubules. In addition to the expression in kidney, claudins are also detected in other organs and tissues [4]. For instance, claudin-11 is highly expressed in the testis [12] and claudin-19 is found in the Schwann cells [13]. The expression of claudins in different organs

*Corresponding author. Fax: +852 2819 9636.
E-mail address: jmluk@hkucc.hku.hk (J.M. Luk).

appears to be crucial on development and cellular physiology. It is noted that claudin-6 is present in embryonic epithelia and is shown to have a role in epithelial cell differentiation [14]. The significance of claudins in kidneys is clearly illustrated in human patients with hypomagnesemia hypercalciuria syndrome, which is caused by claudin-16 defects [15]. Based on the variety and specificity of claudins in kidneys, we speculated the presence of other unidentified claudins in the kidney to regulate paracellular conductance and/or maintain renal homeostasis. The present study has characterized a newly identified claudin-19 with implications in renal physiology.

2. Materials and methods

2.1. Animals

Sprague–Dawley rats were obtained from the Laboratory Animal Unit (The University of Hong Kong, Hong Kong). BALB/cByJ mice were purchased from Jackson Laboratory (Bar Harbour, ME). Animals were housed individually in a pathogen-free ventilation cage at the veterinary care facility of the Experimental Animal Surgery laboratory. The conductions of animal experiments were approved by the guidelines set forth by the University's Committee on Using Live Animals for Teaching and Research. Kidneys were collected from rats and mice in different postnatal ages (day 15, day 45 and adult). The dissected tissues were immediately preserved in buffered formalin for histological examinations.

2.2. Clinical samples

Surgically resected and postmortem polycystic kidney specimens were selected from archival materials filed in the Department of Pathology, Queen Mary Hospital, Hong Kong. Clinical history of patients was reviewed by renal pathologist (KWC) to confirm the diagnosis of autosomal dominant polycystic kidney disease. Normal kidney tissues were selected for control from archival autopsy materials, as previously described [16]. Tissues were fixed in buffered 10% formalin, routinely processed and embedded in paraffin blocks.

2.3. RACE cloning of mouse claudin-19

Molecular cloning of mouse claudin-19 was done by RACE using the Marathon-ready cDNA library (Clontech, Palo Alto, CA). For the 5′-RACE experiments, mouse kidney Marathon-ready cDNA was subjected to two consecutive rounds of PCR as described by manufacturer's instructions using adaptor primer (AP) 1 and claudin-19 anti-sense (Cld-19-AS) primers (5′-CCAGGGCCAGGAGTGA-ATCGTAGAGT-3′). 1 μl of one-tenth diluted PCR product was used for the second round of PCR using AP 2 and Cld-19-AS nested primer (5′-CGCAAGACATCCACAGCCCTTCGTAG-3′). PCR products were subsequently cloned into the pTOPO2.1 vector (Invitrogen, Carlsbad, CA) and sequenced using M13 primer. For the 3′-RACE experiment, Cld-19-S (5′-AATTTGGCCCAGCTCTGTTCGTCG-3′) and Cld-19-S nested primers (5′-AGGGCGAACAGCATCCCACA-GC-3′) were used instead. Sequences were assembled using the DNasis version 2.1 program (Hitachi Software Engineering, San Bruno, CA) and submitted to a BLAST analysis for identification.

2.4. Phylogenetic analysis on claudin-19

Multiple sequence alignment of cldn19 genes in different species and generation of phylogenetic tree of the mouse claudin family were carried out using ClustalW program (http://www.ebi.ac.uk/clustalw/)[17]. Presentation of the alignment was performed using the BoxShade 3.21 program (http://www.ch.embnet.org/software/BOX_form.html).

2.5. Northern blot analysis

The expression levels of cldn19 mRNA in various mouse and rat tissues were examined by using multi-tissue Northern blots (Seegene Inc., Seoul, Korea). A 307 bp PCR fragment corresponding to mouse claudin-19 was amplified using moCld-19-S (5′-CACTCCTGGC-CCTGGACGGTCATAT-3′) and moCld-19-AS (5′-AGGCCCAGC-CGACGAACAGA-3′) primers. DNA fragment was radiolabeled
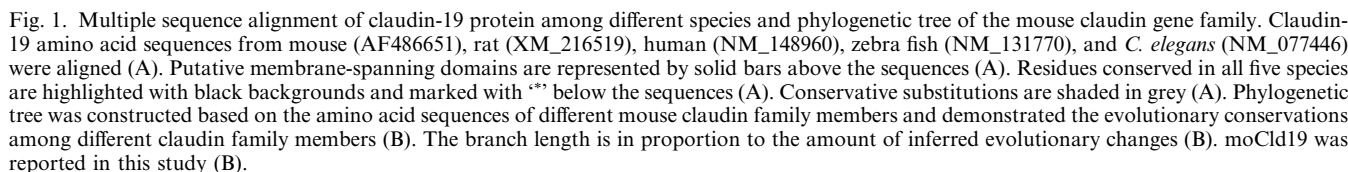
with α-[^{32}P]-dCTP (DuPont NEN, Boston, MA) using Rediprime II DNA labelling system (Amersham, Piscataway, NJ) and purified by spin columns (Princeton Separations, Adelphia, NJ) as described [18]. In brief, membranes were pre-hybridized with Rapid-hyb buffer (Amersham) at 65 °C for 2 h. Hybridizations were performed at 65 °C for 18 h in the Rapid Hyb-buffer containing radioactive probes (1×10^6 cpm). Membranes were washed once in 2× SSC, 0.1% SDS and once in 1× SSC, 0.1% SDS each at 45 °C for 20 min before subjected to autoradiography for 12–48 h. Hybridization signals were captured using BioMax autoradiography film (Eastman Kodak, Rochester, NY).

2.6. RT-PCR

Semi-quantitative RT-PCR was performed as in previously described procedures [19,20] to determine the relative expressions of cldn19 in different organs and tissues. Briefly, total RNA from frozen tissues was prepared using the RNeasy Mini Kit (Qiagen, Valencia, CA) and converted into cDNA using Superscript II RNase H- reverse transcriptase and oligo(dT)$_{12–18}$ primer (Gibco-Invitrogen, Carlsbad, CA). Mouse β-actin (sense primer: 5′-AGCCATGTACGTAGC-CATCC-3′; anti-sense primer: 5′-CTCTCAGCTGTGGTGGTGAA-3′; product size: 350 bp), claudin-19, and glyceraldehyde-3-phosphate dehydrogenase (GAPDH) (sense primer: 5′-ACCACAGTCCATGC-CATCAC-3′; anti-sense primer: 5′-TCCACCACCCTGTTGCTGTA-3′; product size: 470 bp) primers were used for PCR. In brief, 5 μl of cDNA was mixed with 45 μl 1× PCR reaction buffer (10 mM Tris–HCl; pH 9.0, 50 mM KCl, 1.5 mM MgCl$_2$, and 0.1% Triton X-100), containing 200 nM primers, 200 μM dNTPs, and 5 U Taq DNA polymerase (Roche, Palo Alto, CA). Preliminary experiments were performed to determine the linearity of the PCR products by using different concentrations of primers and cDNA. Different temperatures and cycles of the PCR were carried out also [20]. PCR conditions were 30 cycles of 94 °C for 40 s, 64 °C for 30 s, and 72 °C for 40 s, which was followed by a final extension at 72 °C for 10 min. The housekeeping β-actin and GAPDH gene were used as the internal control and for normalization of the PCRs. Parallel samples with no reverse transcriptase served as the RT-ve control. The amplified PCR products were separated on a 2% agarose gel, stained with ethidium bromide and visualized by UV illumination. The gel images were captured and the relative changes of PCR products were quantified by Syngene CCDBIO Acquisition and Analysis Software (Hitachi Genetics System, Alameda, CA).

2.7. Immunohistochemical localizations of claudin-19 in MDCK I cells and kidney tissues

Immunocytochemistry and immunohistochemistry were performed as described [21]. In brief, $\sim 1 \times 10^4$ MDCK I cells (ATCC, Manassas, VA) grown on coverslips were fixed with ice-cold methanol/acetone (v/v; 1:1) and rehydrated in PBS. After incubating in 3% bovine serum albumin (BSA) (w/v in PBS) for 1 h, sections were incubated with rabbit anti-claudin-19 polyclonal antibody (#7161) (1:100), which was synthesized by Alpha Diagnostic (San Antonio, TX) and raised against the claudin-19 peptide sequence flanking amino acids 23–39 (ASTA-LPQWKQSSYAGDAC) (Fig. 1) or rabbit anti-zonula occludens-1 (ZO-1) polyclonal antibody (1:200) (Zymed, South San Francisco, CA). After that, sections were incubated with species-matched FITC-conjugated secondary antibody (1:50; in 3% BSA/PBS) (Zymed) for 30 min at room temperature. After DAPI (Molecular Probes, Eugene, OR) counterstain, slides were mounted with Vectashield medium (Vector Laboratories, Burlingame, CA). Images were examined with Nikon epifluorescent upright microscope E600 (Nikon, Tokyo, Japan) and captured with a 3-CCD color camera DC-330 (DAGE-MTI, Michigan City, IN). For immunohistochemistry, paraffin tissue sections were cut at 4-μm thick and endogenous peroxidase activity was blocked with 0.3% hydrogen peroxide (v/v in methanol). BSA blocking and primary antibody incubation were the same as those described above. Both aquaporin (AQ)-1 and AQ-2 antibodies were commercially available (Calbiochem, San Diego, CA) and used at a dilution of 1:500 in 2% BSA. After that, sections were incubated with horseradish peroxidase (HRP)-conjugated anti-rabbit antibodies (Zymed) for 1 h at room temperature. The localizations of claudin-19, AQ-1, AQ-2, and ZO-1 were visualized using 3,3-diaminobenzidine tetrahydrochloride (DAB) (Zymed). For negative controls, peptide-neutralized antibody or rabbit immunoglobulin G (IgG) (1:500) were used.

Fig. 1. Multiple sequence alignment of claudin-19 protein among different species and phylogenetic tree of the mouse claudin gene family. Claudin-19 amino acid sequences from mouse (AF486651), rat (XM_216519), human (NM_148960), zebra fish (NM_131770), and *C. elegans* (NM_077446) were aligned (A). Putative membrane-spanning domains are represented by solid bars above the sequences (A). Residues conserved in all five species are highlighted with black backgrounds and marked with '*' below the sequences (A). Conservative substitutions are shaded in grey (A). Phylogenetic tree was constructed based on the amino acid sequences of different mouse claudin family members and demonstrated the evolutionary conservations among different claudin family members (B). The branch length is in proportion to the amount of inferred evolutionary changes (B). moCld19 was reported in this study (B).

2.8. Immunoprecipitation and SDS–PAGE

Immunoprecipitation and western blot were performed as previously described [20,22]. MDCK cells were grown to monolayer in a 100 mm culture dish. Total cell lysates were extracted using lysis buffer (20 mM Tris, 0.15 M NaCl, 2 mM EDTA, 10% glycerol, 1% NP-40, 1 mM PMSF at pH 7.4) as described [20]. 500 μg cell lysates were first precleared using 50 μl protein A (Amersham) for 2 h at 4 °C with agitation. Precleared lysates were incubated with either antibodies (claudin-19 or ZO-1) or preimmune normal rabbit serum (NRS) as a negative control overnight at 4 °C with agitation before the addition of 100 μl protein A to precipitate the immunocomplexes. After washing with lysis buffer, proteins were eluted by boiling the immuno-precipitates at 100 °C for 7 min in a denaturing sample buffer with 2-mercaptoethanol. Eluted proteins were resolved by running a 5% SDS–PAGE. After electro-transfer to PVDF membrane, target proteins were detected by chemiluminescence using ECL western blotting detection kit (Amersham).

3. Results

3.1. Molecular cloning and characterization of claudin-19 cDNA

The 675 bp *cldn19* cDNA was amplified in RACE reactions (GenBank Accession No.: AF486651). It encoded a 224 amino

acid protein with a calculated molecular weight of 23.8 kDa (Fig. 1A). The gene was mapped to the mouse chromosome 4. The *cldn19* gene contained five exons with a huge intron between exon 3 and exon 4. Hydrophilicity analysis (TMHMM v2.0) predicted that like other claudins, claudin-19 contained four transmembrane domains with both intracellular N- and C-terminus (Fig. 1A). The first putative extracellular loop was longer than the second putative extracellular loop (Fig. 1A). Multiple amino acid sequence alignments among different species (mouse, rat, human, zebra fish, and *C. elegans*) were carried out (Fig. 1A). Mouse claudin-19 shared 98.2% and 95% amino acid identities with rat and human counterparts, respectively, and to much less extent with zebra fish and *C. elegans* (Fig. 1A).

3.2. Phylogenetic and tissue distribution of claudin-19

The deduced amino acid sequence of mouse claudin-19 and amino acid sequences of other mouse claudin members were used to construct the phylogenetic tree (Fig. 1B). Claudin-19 was found on the same root of the phylogenetic tree of claudin-1 and -7, which shared 73% and 75% similarity with claudin-19, respectively (Fig. 1B). Mouse *cldn19* mRNA transcript (~1.0 kb) was exclusively expressed in the kidney by Northern blot analysis (Fig. 2A). The same probe was used to detect claudin-19 in rat tissues, and similar tissue expression pattern was obtained (Fig. 2B). Semi-quantitative RT-PCR method was employed to further examine the expression profile of claudin-19 in mouse (Fig. 2C) and rat (Fig. 2D) tissues. Thus, claudin-19 was abundantly detected in the kidney tissue, and with much weaker expression in the brain as well (Fig. 2C and D). Actin (Fig. 2C) and GADPH (Fig. 2D) were used as positive controls in PCR.

3.3. ZO-1 is associated with claudin-19-containing protein complexes at the junction sites in MDCK cell

Immunoreactive claudin-19, which appeared as green immunofluorescence, was found at the junction sites in confluent MDCK cell monolayers (Fig. 3A and B), similar to the localization of ZO-1 (Fig. 3C and D). No immunofluorescent signal was detected with the corresponding IgG isotype control in the parallel experiments (Fig. 3E and F). Due to their close proximity in the localizations in MDCK cell monolayers, immunoprecipitation was performed to investigate whether ZO-1 is part of the protein complexes with claudin-19, and indeed, a putative associated adaptor in the claudin-19-containing protein complexes (Fig. 3G).

3.4. Localizations of claudin-19, AQ-1, AQ-2, and ZO-1 in human, rat, and mouse kidney

Aquaporin-1 (AQ-1) is a marker for the proximal tubules and descending thin limbs of loop of Henle, whereas aquaporin-2 (AQ-2) is specific for the collecting ducts [23]. These two markers and the morphological structures of the kidney were used to determine the localization of claudin-19 in kidneys. In the cortex, the distal tubules were recognized as AQ-1 and AQ-2 double-negative tubules surrounding the glomerulus, whereas the collecting ducts contained AQ-2 staining only but not AQ-1. Representative immunohistochemical staining for claudin-19, AQ-1, and AQ-2 in serial sections of human kidneys are shown in Fig. 4. Peptide-pre-absorbed controls for both aquaporin antibodies were preformed, which yielded no positive reaction in the sections (data not shown). The present immunohistochemical findings indicated that claudin-19 was predominantly expressed in the distal tubules, albeit much lesser extent in the proximal tubules, in the cortex of rat,
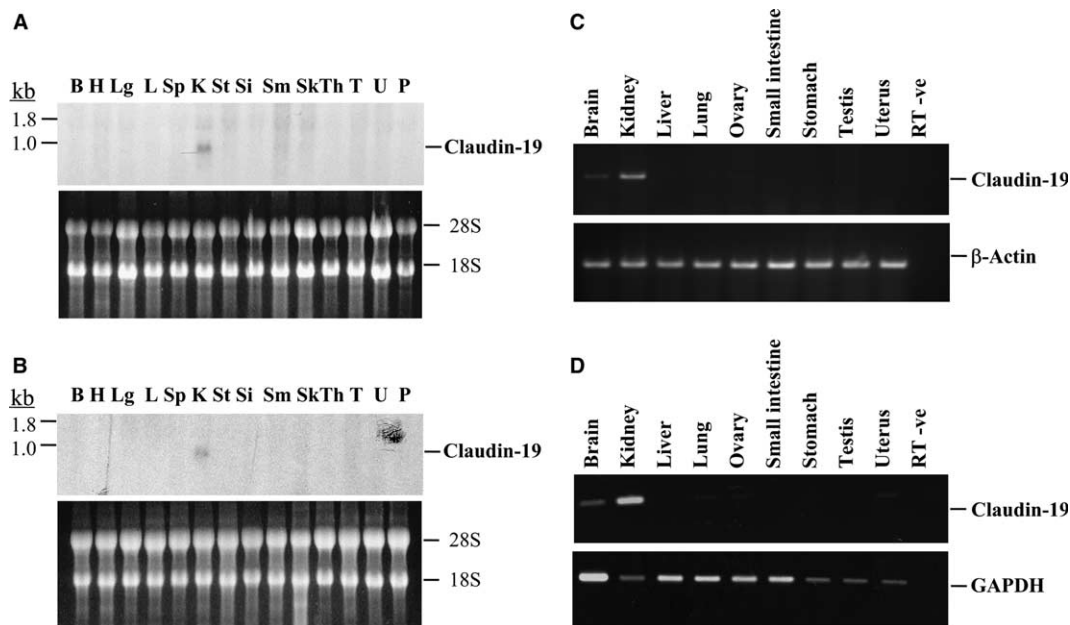

Fig. 2. Expression of claudin-19 mRNA in mouse and rat tissues. Mouse (A) and rat (B) multi-tissue Northern blots were hybridized with mouse claudin-19 DNA probes. Each lane contained 20 µg of total RNA from different mouse (A) or rat (B) tissues (B, brain; H, heart; Lg, lung; L, liver; Sp, spleen; K, kidney; St, stomach; Si, small intestine; Sm, skeletal muscle; Sk, skin; Th, thymus; T, testis; U, un-pregnant uterus; P, placenta). A band with size of ~1.0 kb corresponding to claudin-19 was detected in both mouse and rat Northern blots. RNA gel stained with ethidium bromide was used as a loading control (A and B). The expressions of claudin-19 mRNA in mouse (C) and rat (D) tissues were assayed by semi-quantitative PCR. A PCR product of size 307 bp representing the presence of claudin-19 was detected. RNA in different organs and tissues were normalized using β-actin (C) or GAPDH (D), the house-keeping genes.
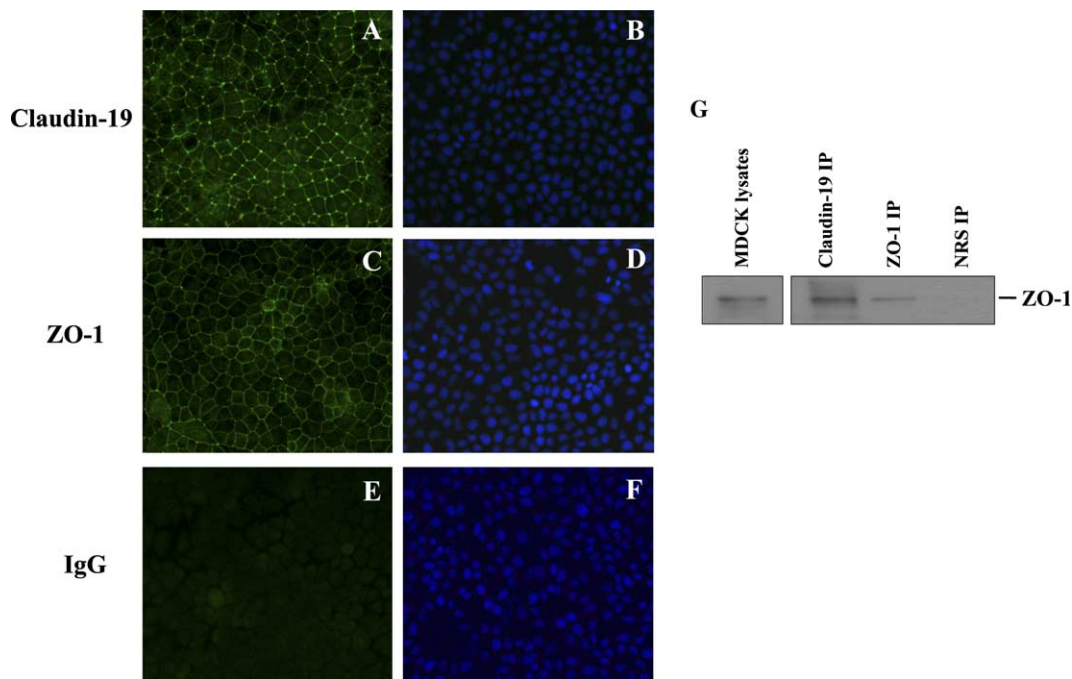
Fig. 3. Immunofluorescence cytochemistry and immunoprecipitation of claudin-19 and ZO-1 in MDCK cell monolayers. Immunoreactive claudin-19 (A) and ZO-1 (C), appeared as green immunofluorescence, were detected by immunofluorescent microscopy. No signal was found when the corresponding IgG was used (E). The nuclei of MDCK cells were counter-stained with DAPI for visualizations (B, D, and F). Magnification (A–F): 200×. Immunoprecipitation was performed using claudin-19 antibody, ZO-1 antibody, and preimmune NRS to investigate whether ZO-1 is a binding partner of claudin 19-associated protein complex in MDCK cells (G). MDCK lysate without carrying out immunoprecipitation was run in parallel lane for the identification of the target ZO-1 band on western blot (G). NRS IP denoted the negative control of claudin-19 immunoprecipitation, which used the pre-immune NRS in place of the primary antibody.

mouse, and human kidneys (Fig. 4). In the medulla region, claudin-19 was largely expressed in the collecting ducts with mild expressions in the loop of Henle (Fig. 4). The results were read and confirmed by certified renal pathologist (KWC). The expressions of both claudin-19 (Fig. 5A–C) and ZO-1 (Fig. 5E–G) were detected in developing kidneys isolated from postnatal day 15, day 45, and adult mouse kidneys. Similar expression patterns were observed in rat kidneys for claudin-19 (Fig. 5I–K) and ZO-1 (Fig. 5M–O). From day 45 onwards, brown immunoprecipitates corresponding to the localizations of claudin-19 (Fig. 5B and C) and ZO-1 (Fig. 5F and G) were specifically detected in mouse kidneys. Similar localizations were observed in rat kidney sections for claudin-19 (Fig. 5J and K) and ZO-1 (Fig. 5N and O). Surprisingly, prominent localizations of claudin-19 (Fig. 5A–C and I–K) and ZO-1 (Fig. 5E–G and M–O) were also found in the nuclei. By contrast, no positive signal was detected in control sections incubated with peptide pre-absorbed antibody in parallel control experiments (Fig. 5D, H, L, and P).

3.5. Expressions of claudin-19 and ZO-1 in normal and polycystic human kidneys

Immunoreactivity of claudin-19 (Fig. 6A) and ZO-1 (Fig. 6C) were found to localize at the apical and basolateral junction sites between neighbouring cells and lumen linings in the renal tubules in human kidneys. Junctions, cytoplasm, and nuclei were stained positive for claudin-19, similar to the localizations of claudin-19 and ZO-1 in rat and mouse kidneys (Fig. 5). Interestingly, some very intense staining (both claudin-19 and ZO-1) was found in the nuclei of the cells in healthy

human kidney. In polycystic kidneys, the renal cyst epithelia demonstrated decreased expression and variable localization of claudin-19 with diffuse staining pattern throughout the cytoplasm (Fig. 6B). Likewise, ZO-1 also yielded dyslocalization in polycystic human kidney (Fig. 6D). However, minimal localization of ZO-1 was still found at the apical junction sites in polycystic human kidney (Fig. 6D). By contrast, immunoreactivty of claudin-19, but not ZO-1, was still observed in the nuclei in polycystic human kidney.

4. Discussion

The present study described the molecular cloning and characterization of a newly identified TJ gene (cldn19) that is predominantly expressed in mouse and rat kidneys. Phylogenetic analysis demonstrated that claudin-1 and -7 are in the same evolutionary branch of claudin-19, postulating that these three claudins share similar structural features and functional roles. Although the three claudins are positively identified in kidneys by Northern blot analysis in this and other study [7], they exhibit distinct and overlapping renal distributions. Claudin-1 and -7 are found in the high-resistant part of nephrons (collecting ducts and distal tubules) and low-resistant renal segments (proximal tubules and glomerulus) [7,8,24]. By contrast, localizations of claudin-19 are predominantly expressed in the high-resistant segments of nephrons, having an important function for the reabsorption of Ca^{2+}, Mg^{2+}, and water [25,26] and suggestion that claudin-19 could be an essential cation transporter in 'tighter' renal epithelium. This notion is further supported by
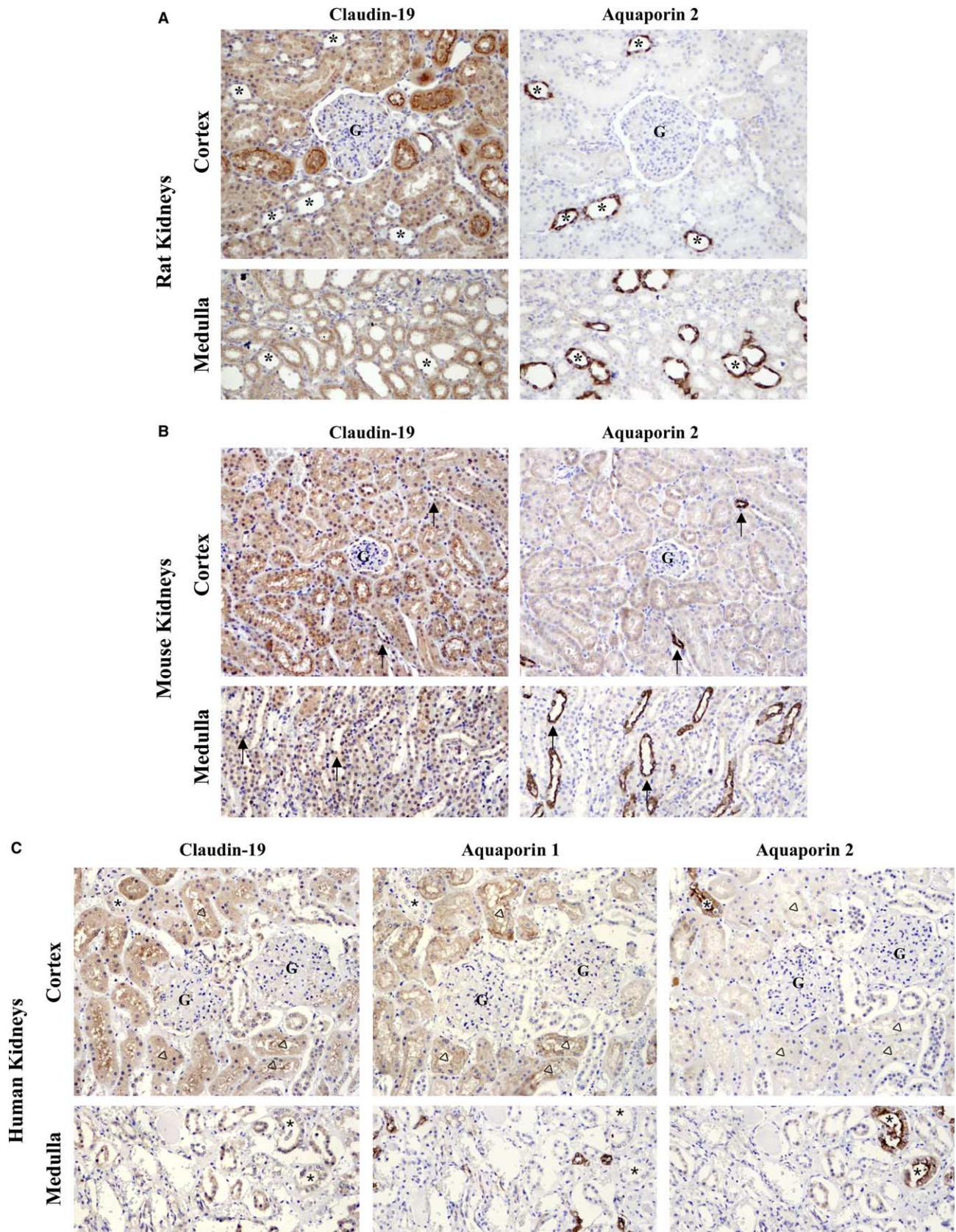
Fig. 4. Localizations of claudin-19 in the cortex and medulla of the kidneys. Rat, mouse, and human serial consecutive kidney sections were stained for the presence of claudin-19, aquaporin-1, and aquaporin-2 using immunohistochemistry. Stars, arrows, and open triangles denoted the corresponding renal tubules in the serial sections stained for different antibodies for comparisons. Glomerular structures were annotated with letter "G".
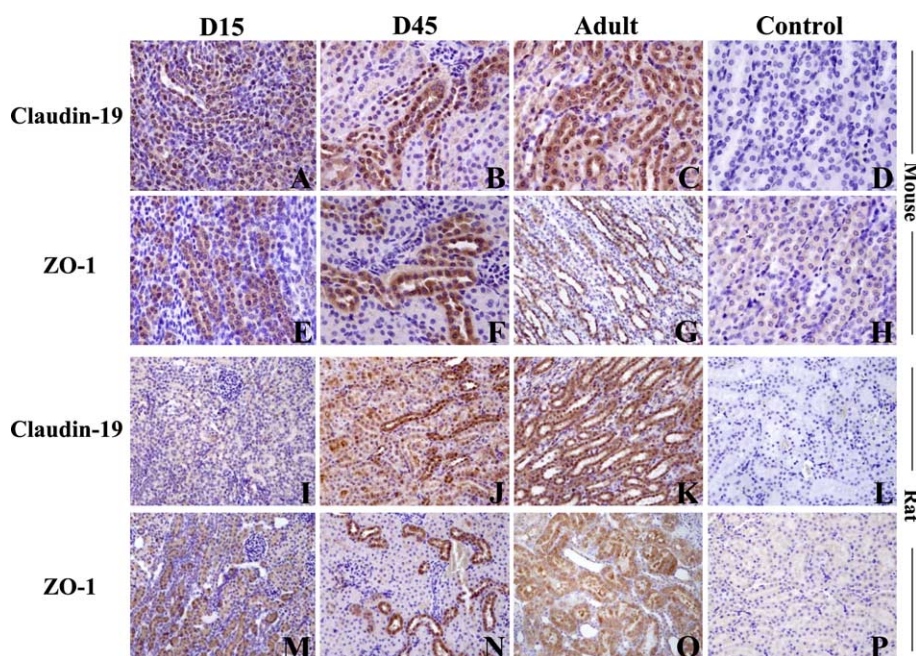
Fig. 5. Localizations of claudin-19 and ZO-1 in mouse and rat kidneys by immunohistochemistry. Mouse (A–H) and rat (I–P) kidney sections were stained with claudin-19 (A–C and I–K) and ZO-1 (E–G and M–O) antibodies at postnatal day 15 (D15), day 45 (D45), and adult. Brown signs corresponded to the localizations of claudin-19 and ZO-1 in the kidney tubules. Control sections were stained with the same antibodies pre-absorbed with peptide for claudin 19 or NRS for ZO-1. Magnification: 200×.
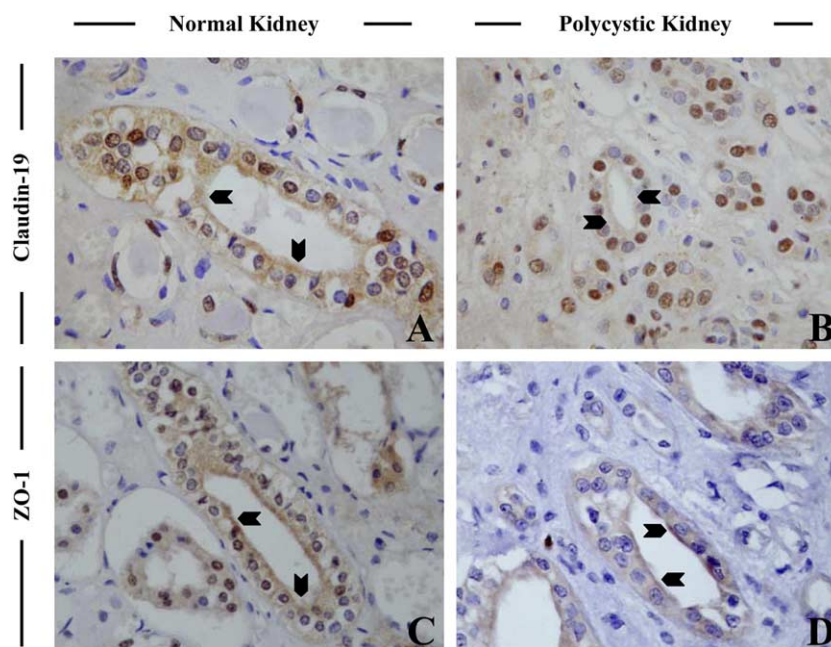

Fig. 6. Expression patterns of claudin-19 and ZO-1 in normal and polycystic human kidneys. Localizations of claudin-19 (A and B) and ZO-1 (C and D) in healthy (A and C) and polycystic (B and D) human kidneys were examined by immunohistochemistry as described. Magnification: 200×.

the presence of claudin-19 at the junction sites in MDCK I cell monolayers, which also express claudin-1 (a claudin in the high electrical resistant renal segments), but not claudin-2 (a claudin in low electrical resistant renal segments) [9,11,24]. While water reabsorption in kidneys is mainly coordinated by aquaporins [27], claudin-19 is speculated to have complementary roles in adjusting the cationic paracellular conductance along these seg-ments. On the other hand, claudin-7 and claudin-19 demon-strate distinct cellular localizations. Claudin-7 is highly concentrated at the basolateral membrane [8], whereas clau-din-19 is found mainly in the renal lumen linings, with slight expression in the basolateral sites, in this study. These findings suggest that claudin-19 complements the roles of other claudins in the kidneys.

Deduced amino acid sequence analysis reveals the structural and functional diversity among claudin-1, -7, and -19. Both the amino acid sequences of the C-termini of mouse claudin-1 (Accession No.: O88551) and -7 (Accession No.: NP_058583) are ended in YV, a site that has been shown to bind PDZ domain-containing proteins [28], including ZO family members, which are adaptors at the site of TJ [4]. However, the C-terminus of claudin-19 is terminated in GV amino acid residues. Unexpectedly, claudin-19 still appeared to be associated with ZO-1 at the junction sites in MDCK I cell monolayers and is found to be in a protein complex comprising of at least ZO-1 by immunoprecipitation. This suggests that ZO-1 either directly binds to claudin-19 or is in the proximity of claudin-19 via bindings with other claudin members, such as claudin-1 that has been shown to co-localize with ZO-1 in MDCK cells [11] and possesses C-terminal YV amino acid residues [1]. However, a recent study demonstrated that ZO-1 also binds to the C-terminus of claudin-16, which ends in TRV amino acids instead of YV residues [29], suggesting the diversified ZO-1-binding sites of claudins. Claudin-ZO-1 binding is significant for the functions of claudins. As demonstrated in claudin-16 mutation, an inactivation of PDZ-binding motifs in claudin-16 and subsequent ZO-1 dissociation leads to childhood hypercalciuria [30]. As such, these observations open the possibility of claudin-19/ZO-1 interactions and also suggest the presence of other putative binding partners of claudin-19.

Besides, claudin-19, there are claudin-1, -3, -4, -7, -8, and -16 also residing in the distal tubules and collecting ducts [7,8,15,24], and their roles in paracellular transport of cations in the renal tubules have been demonstrated [31]. The biological importance of these claudin members in renal and other organ have been clearly demonstrated in mutants and gene-targeting studies [32]. For instance, claudin-16 mutations lead to defects in renal ion homeostasis, resulting in the development of hypomagnesemia and hypercalciuria [15]. For other claudins that are found in the distal tubules and collecting ducts, their mutations also associate with defects in other organs [32]. Since these claudins are highly expressed in other organs and not restricted in kidneys, no report has illustrated any renal dysfunction due to their associated mutations [32]. Because claudin-19 was highly expressed in kidneys, any malfunctions and mutations of this TJ molecule may lead to renal disorders. Mutations of proteins with significant functions are commonly associated with diseases. In kidneys, mutations in claudin-16, which is restrictedly expressed in the thick ascending limb of Henle and distal convoluted tubule, lead to hypomagnesemia with hypercalciurai and childhood hypercalciuria [15,30]. Herein, claudin-19 demonstrated decreased expression and altered localizations in polycystic human kidney. Expression of claudin-19 at the tubule lumen linings was significantly diminished in polycystic kidney tissue when compared to the healthy kidney counterparts. Clinical symptoms of polycystic kidney disease include the development of fluid-filled cysts in affected kidneys. Lack of cell surface E-cadherin and sequestrations of E-cadherin in intracellular pool were also reported in polycystic kidney cells [33], similar to the present observations of claudin-19 in polycystic kidneys. These findings suggest the interrelationship between claudin-19 and E-cadherin, probably via polycystin in the manifestations of polycystic kidney diseases. Besides, increasing evidences have consolidated the inter-correlation between AJ and TJ proteins [34].

In view of predominant expression of claudin-19 in kidneys, it is suggested that claudin-19 shares significant roles with other claudin molecules in regulating the paracellular transport and homeostasis in kidneys. Despite that, our recent study has demonstrated that the promoter region of *cldn19* gene is structurally different from other claudin members, and presumably, its expression is under different regulatory mechanism [35]. Other important questions including the specific role of claudin-19 in regulating TJ function in the distal tubules and collecting duct and how its expression is downregulated in polycystic kidneys are under investigation.

References

[1] Schneeberger, E.E. and Lynch, R.D. (2004) The tight junction: a multifunctional complex. Am. J. Physiol. Cell Physiol. 286, C1213–C1228.

[2] Fanning, A.S., Mitic, L.L. and Anderson, J.M. (1999) Transmembrane proteins in the tight junction barrier. J. Am. Soc. Nephrol. 10, 1337–1345.

[3] Bazzoni, G. (2003) The JAM family of junctional adhesion molecules. Curr. Opin. Cell. Biol. 15, 525–530.

[4] Gonzalez-Mariscal, L., Betanzos, A., Nava, P. and Jaramillo, B.E. (2003) Tight junction proteins. Prog. Biophys. Mol. Biol. 81, 1–44.

[5] Anderson, J. (2001) Molecular structure of tight junctions and their role in epithelial transport. News Physiol. Sci. 16, 126–130.

[6] Claude, P. and Goodenough, D.A. (1973) Fracture faces of zonulae occludentes from "tight" and "leaky" epithelia. J. Cell Biol. 58, 390–400.

[7] Kiuchi-Saishin, Y., Gotoh, S., Furuse, M., Takasuga, A., Tano, Y. and Tsukita, S. (2002) Differential expression patterns of claudins, tight junction membrane proteins, in mouse nephron segments. J. Am. Soc. Nephrol. 13, 875–886.

[8] Li, W.Y., Huey, C.L. and Yu, A.S.L. (2004) Expression of claudin-7 and -8 along the mouse nephron. Am. J. Physiol. Renal Physiol. 286, F1063–F1071.

[9] Enck, A.H., Berger, U.V. and Yu, A.S.L. (2001) Claudin-2 is selectively expressed in proximal nephron in mouse kidney. Am. J. Physiol. Renal Physiol. 281, F966–F974.

[10] Richardson, J.C., Scalera, V. and Simmons, N.L. (1981) Identification of two strains of MDCK cells which resemble separate nephron tubule segments. Biochim. Biophys. Acta 673, 26–36.

[11] Furuse, M., Furuse, K., Sasaki, H. and Tsukita, S. (2001) Conversion of zonulae occludentes from tight to leaky strand type by introducing claudin-2 into Madin–Darby canine kidney I cells. J. Cell Biol. 153, 263–272.

[12] Gow, A., Southwood, C.M., Li, J.S., Pariali, M., Riordan, G.P., Brodie, S.E., Danias, J., Bronstein, J.M., Kachar, B. and Lazzarini, R.A. (1999) CNS myelin and Sertoli cell tight junction strands are absent in Osp/Claudin-11 null mice. Cell 99, 649–659.

[13] Miyamoto, T., Morita, K., Takemoto, D., Takeuchi, K., Kitano, Y., Miyakawa, T., Nakayama, K., Okamura, Y., Sasaki, H., Miyachi, Y., Furuse, M. and Tsukita, S. (2005) Tight junctions in Schwann cells of peripheral myelinated axons: a lesson from claudin-19-deficient mice. J. Cell Biol. 169, 527–538.

[14] Turksen, K. and Troy, T. (2001) Claudin-6: a novel tight junction molecule is developmentally regulated in mouse embryonic epithelium. Dev. Dyn. 222, 292–300.

[15] Simon, D.B., Lu, Y., Choate, K.A., Velazquez, H., Al-Sabban, E., Praga, M., Casari, G., Bettinelli, A., Colussi, G., Rodriguez-Soriano, J., McCredie, D., Milford, D., Sanjad, S. and Lifton, R.P. (1999) Paracellin-1, a renal tight junction protein required for paracellular Mg^{2+} resorption. Science 285, 103–106.

[16] Lee, D.C., Chan, K.W. and Chan, S.Y. (2002) RET receptor tyrosine kinase isoforms in kidney function and disease. Oncogene 21, 5582–5592.

[17] Thompson, J.D., Higgins, D.G. and Gibson, T.J. (1994) CLUSTAL W: improving the sensitivity of progressive multiple sequence alignment through sequence weighting, position-specific gap penalties and weight matrix choice. Nucleic Acids Res. 22, 4673–4680.

[18] Lee, K.F., Yao, Y.Q., Kwok, K.L., Xu, J.S. and Yeung, W.S.B. (2002) Early developing embryos affect the gene expression patterns in the mouse oviduct. Biochem. Biophys. Res. Commun. 292, 564–570.

[19] Luk, J.M., Mok, B.W., Shum, C.K., Yeung, W.S.B., Tam, P.C., Tse, J.Y., Chow, J.F., Woo, J., Kam, K. and Lee, K.F. (2003) Identification of novel genes expressed during spermatogenesis in stage-synchronized rat testes by differential display. Biochem. Biophys. Res. Commun. 307, 782–790.

[20] Lee, N.P.Y., Mruk, D.D., Conway, A.M. and Cheng, C.Y. (2004) Zyxin, axin, and WASP are adaptors that link the cadherin/catenin protein complex to cytoskeleton at adherens junctions in the seminiferous epithelium of the rat testis. J. Androl. 25, 200–215.

[21] Wong, B.W., Luk, J.M., Ng, I.O., Hu, M.Y., Liu, K.D. and Fan, S.T. (2003) Identification of liver-intestine cadherin in hepatocellular carcinoma – a potential disease marker. Biochem. Biophys. Res. Commun. 311, 618–624.

[22] Wang, P.P., Wang, J.H., Yan, Z.P., Hu, M.Y., Lau, G.K., Fan, S.T. and Luk, J.M. (2004) Expression of hepatocyte-like phenotypes in bone marrow stromal cells after HGF induction. Biochem. Biophys. Res. Commun. 320, 712–716.

[23] King, L.S. and Yasui, M. (2002) Aquaporins and disease: lessons from mice to humans. Trends Endocrinol. Metab. 13, 355–360.

[24] Reyes, J.L., Lamas, M., Martin, D., del Carmen Namorado, M., Islas, S., Luna, J., Tauc, M. and Gonzalez-Mariscal, L. (2002) The renal segmental distribution of claudins changes with development. Kidney Int. 62, 476–487.

[25] Imai, M. and Nakamura, R. (1982) Function of distal convoluted and connecting tubules studied by isolated nephron fragments. Kidney Int. 22, 465–472.

[26] Brenner, B.M. () in: Brenner & Rector's the Kidney (Brenner, B.M., Ed.), 7th edn., Saunders, Philadelphia.

[27] King, L.S., Kozono, D. and Agre, P. (2004) From structure to disease: the evolving tale of aquaporin biology. Nat. Rev. Mol. Cell. Biol. 5, 687–698.

[28] Itoh, M., Furuse, M., Morita, K., Kubota, K., Saitou, M. and Tsukita, S. (1999) Direct binding of three tight junction-associated MAGUKs, ZO-1, ZO-2, and ZO-3, with the COOH termini of claudins. J. Cell Biol. 147, 1351–1363.

[29] Ikari, A., Hirai, N., Shiroma, M., Harada, H., Sakai, H., Hayashi, H., Suzuki, Y., Degawa, M. and Takagi, K. (2004) Association of paracellin-1 with ZO-1 augments the reabsorption of divalent cations in renal epithelial cells. J. Biol. Chem. 279, 54826–54832.

[30] Muller, D., Kausalya, P.J., Claverie-Martin, F., Meij, I.C., Eggert, P., Garcia-Nieto, V. and Hunziker, W. (2003) A novel claudin 16 mutation associated with childhood hypercalciuria abolishes binding to ZO-1 and results in lysosomal mistargeting. Am. J. Hum. Genet. 73, 1293–1301.

[31] Yu, A.S.L., Enck, A.H., Lencer, W.I. and Schneeberger, E.E. (2003) Claudin-8 expression in Madin–Darby canine kidney cells augments the paracellular barrier to cation permeation. J. Biol. Chem. 278, 17350–17359.

[32] Mitic, L.L., Van Itallie, C.M. and Anderson, J.M. (2000) Molecular physiology and pathophysiology of tight junctions. I. Tight junction structure and function: lessons from mutant animals and proteins. Am. J. Physiol. Gastrointest. Liver Physiol. 279, G250–G254.

[33] Charron, A.J., Nakamura, S., Bacallao, R. and Wandinger-Ness, A. (2000) Compromised cytoarchitecture and polarized trafficking in autosomal dominant polycystic kidney disease cells. J. Cell Biol. 149, 111–124.

[34] Contreras, R.G., Shoshani, L., Flores-Maldonado, C., Lazaro, A., Monroy, A.O., Roldan, M.L., Fiorentino, R. and Cereijido, M. (2002) E-cadherin and tight junctions between epithelial cells of different animal species. Pflugers Arch. 444, 467–475.

[35] Luk, J.M., Tong, M.K., Mok, B.W., Tam, P.C., Yeung, W.S.B. and Lee, K.F. (2004) Sp1 site is crucial for the mouse claudin-19 gene expression in the kidney cells. FEBS Lett. 578, 251–256.